SUPPORTING INFORMATION

Small CdS nanorods via sacrificial synthesis on perovskite nanocrystals – synthesis and hierarchical assembly

Zuzanna Lawera,† [a] Sylwia Parzyszek,† [a] Damian Pociecha,[a] Wiktor Lewandowski*[a]

[a] Faculty of Chemistry, University of Warsaw, Pasteura 1 St., 02-093 Warsaw, Poland
† Authors contributed equally
E-mail: wlewandowski@chem.uw.edu.pl

TEM characterization of $CsPbBr_3$ perovskites and CdS nanorods.

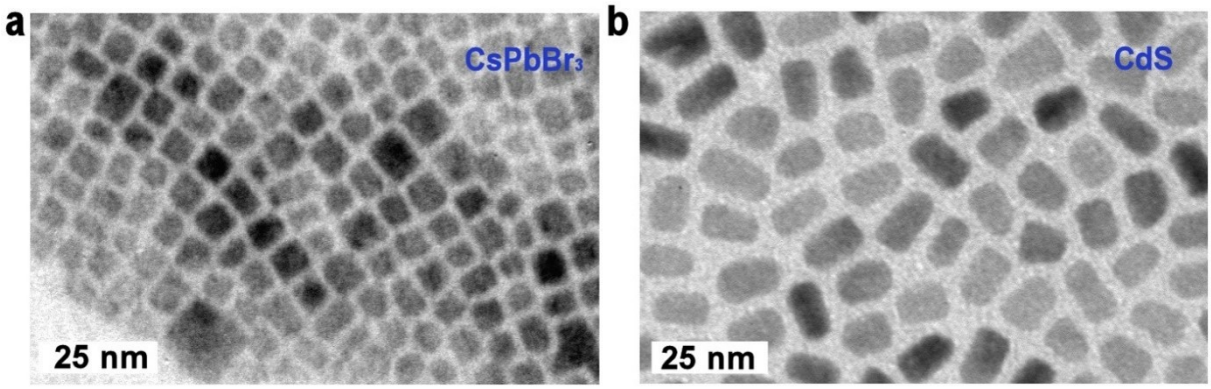

Fig. S 1 TEM images of (a) $CsPbBr_3$ perovskites, and (b) the final CdS NRs.

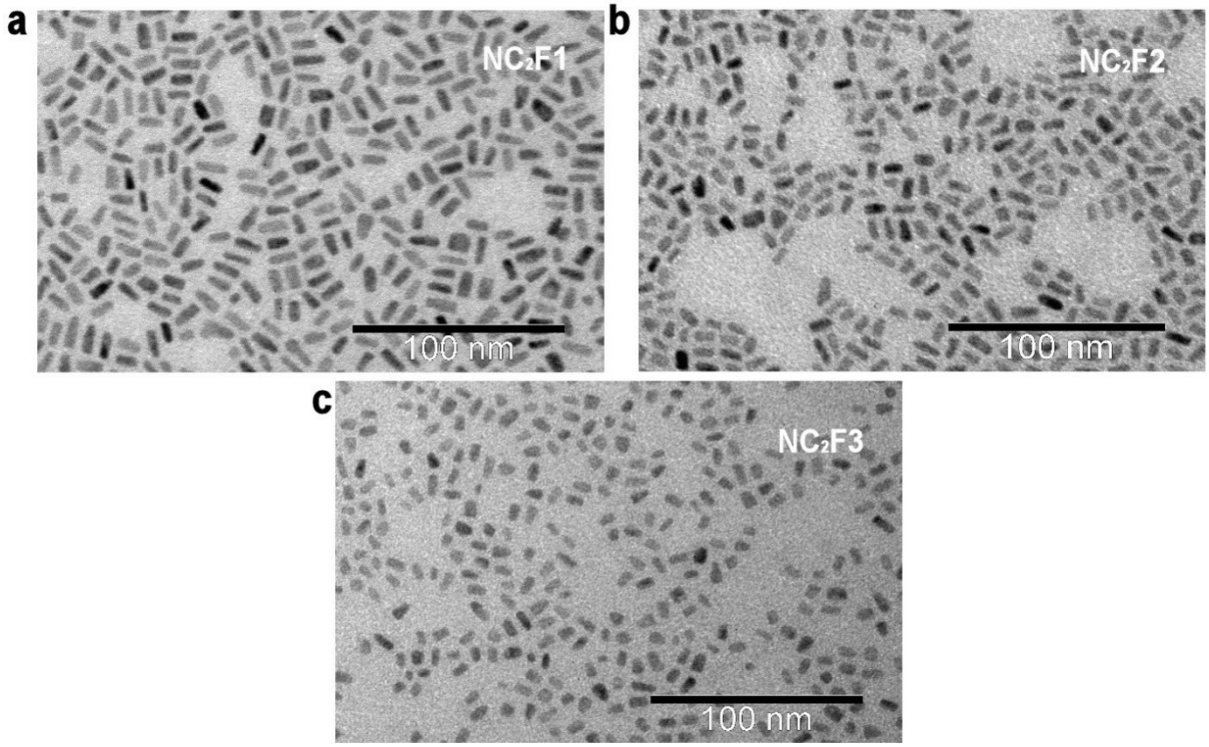

Fig. S 3 TEM images of NC2 (20 min, 180°C) nanocrystals: (a) fraction F1, (b) fraction F2, (c) fraction F3.

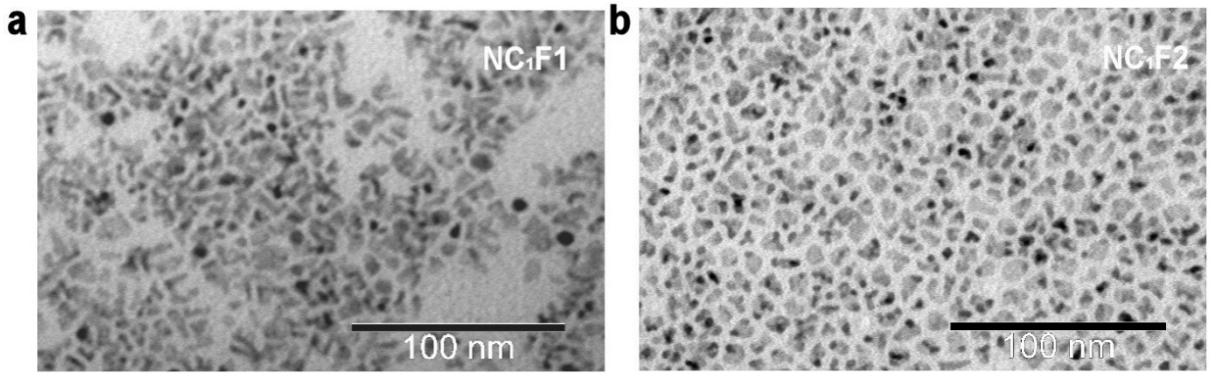

Fig. S 2 TEM images of NC1 (20 min, 150°C) nanocrystals: (a) fraction F1, (b) fraction F2.

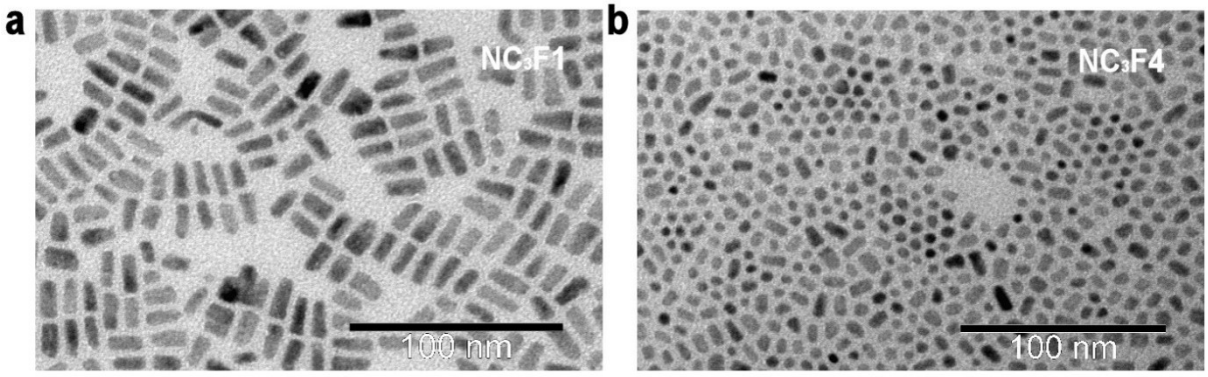

Fig. S 4 TEM images of NC3 (20 min, 230°C) nanocrystals: (a) fraction F1, (b) fraction F2.

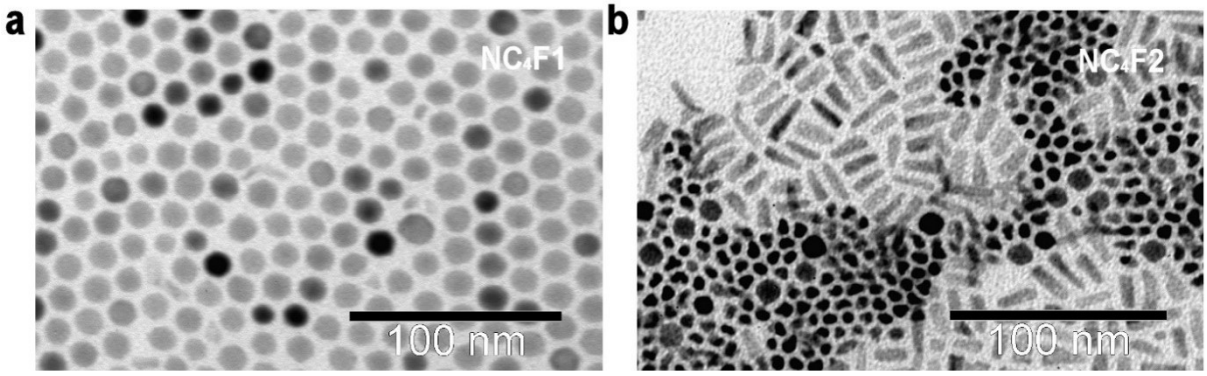

Fig. S 5 TEM images of NC4 (120 min, 150°C) nanocrystals: (a) fraction F1, (b) fraction F2.

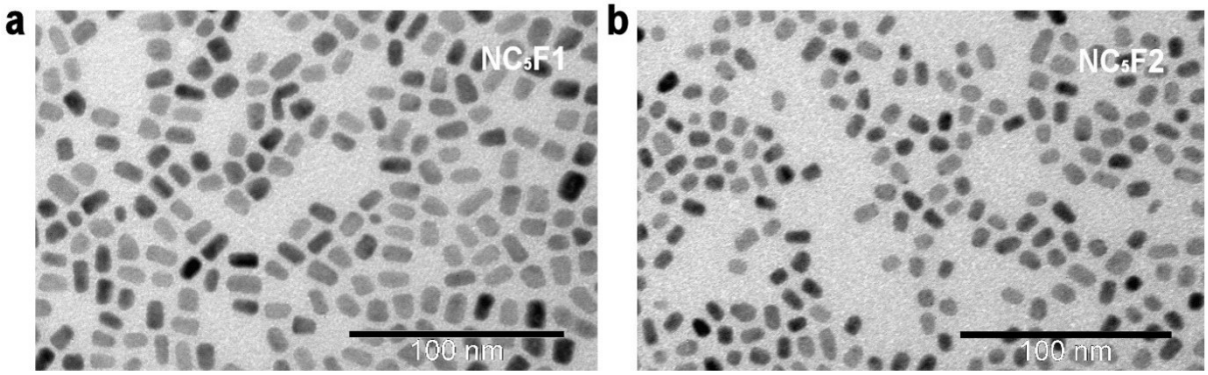

Fig. S 6 TEM images of NC5 (120 min, 200°C) nanocrystals: (a) fraction F1, (b) fraction F2.

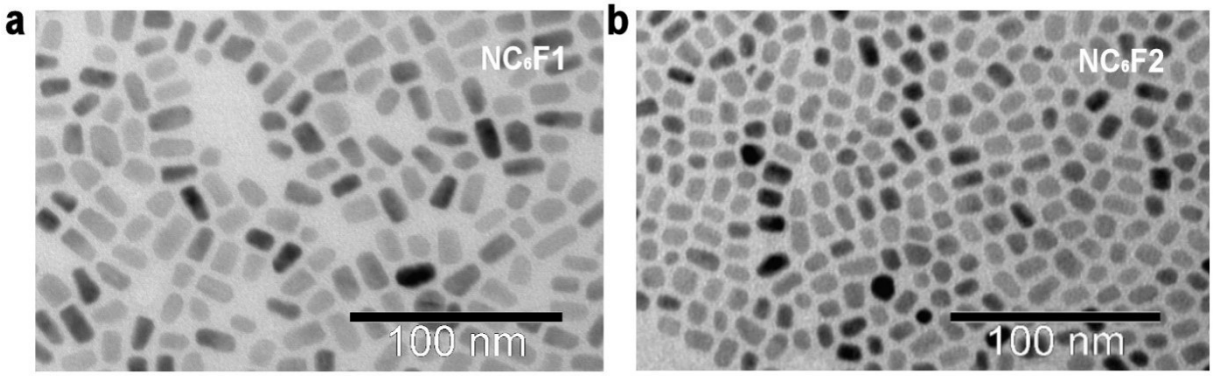

Fig. S 7 TEM images of NC6 (120 min, 250°C) nanocrystals: (a) fraction F1, (b) fraction F2.

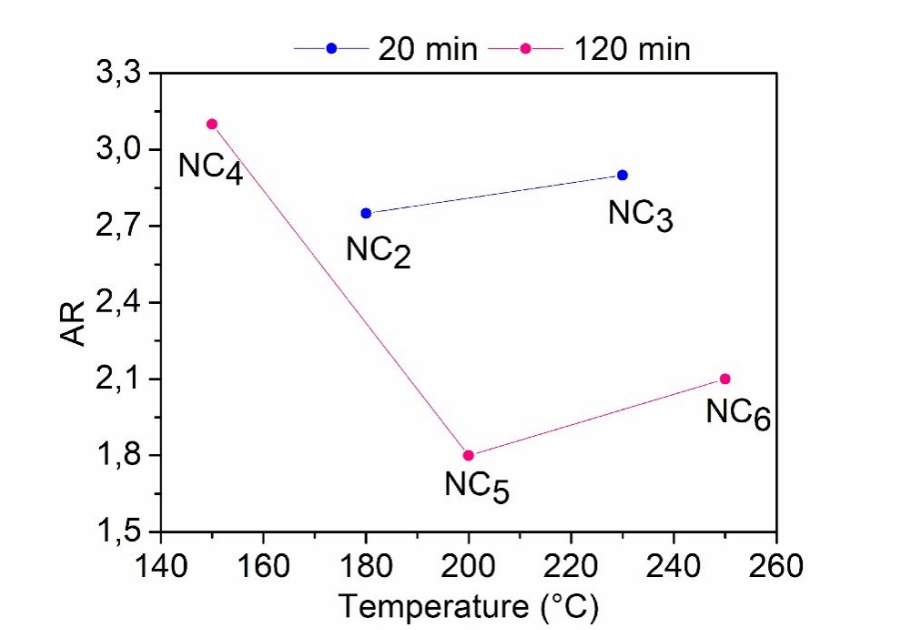

Fig. S 8 Plot presenting the dependence of aspect ratio (AR) on the temperature and time of the reaction. The aspect ratio for nanocrystals NC_1 is undefined due to significant irregularity of shape. The lines are added for eye guidance.

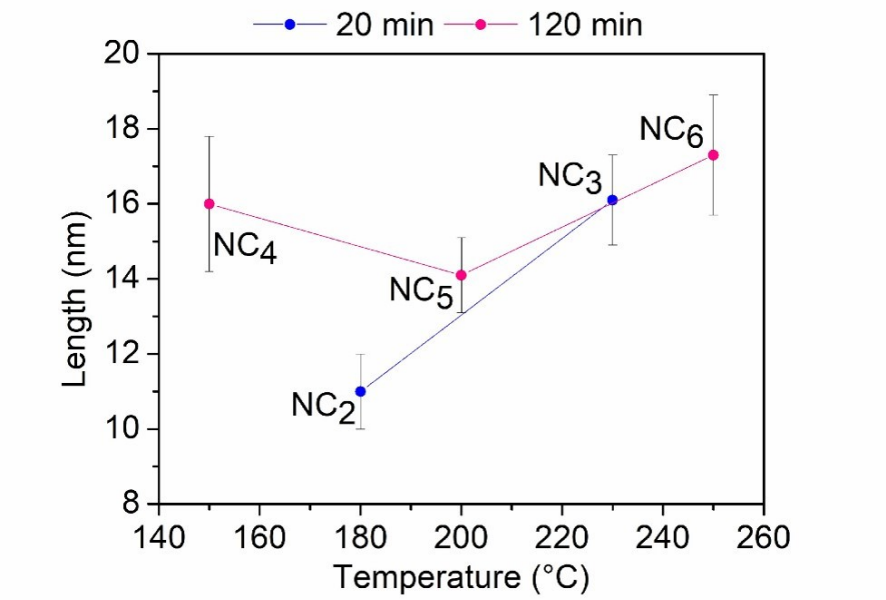

Fig. S 9 Plot presenting the dependence of the size of NCs on the temperature and time of the reaction. Describing nanocrystals NC4 the diameter was measured, and in other cases, the length of nanorods. The lines are added for eye guidance.

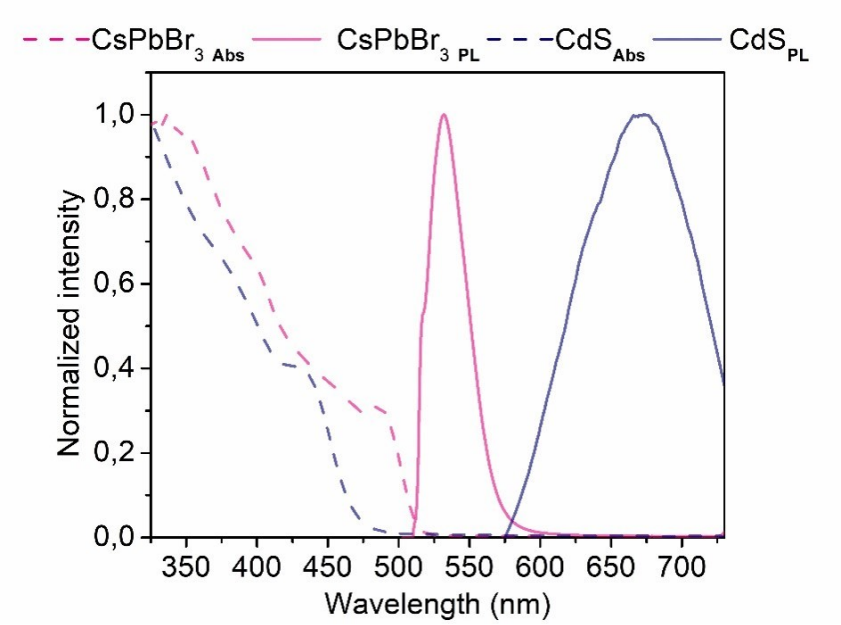

Fig. S 10 UV-Vis and PL spectra of CdS NRs compared with the spectra of CsPbBr3 perovskites obtained in the course of the synthesis and NRs formation, the PL band red-shifts from 532 nm to 672 nm. The extinction main band blue-shifts from 488 nm to 430 nm.

Supplementary note 1. Mechanism of CdS NRs formation

A more in-depth view of the mechanism of the reported synthesis is given below.

I. Examining the reaction products at different stages of reaction conducted at 150°C over 120 min (Fig. S11-S13).

NR4 synthesis was chosen to follow the products of the synthesis at different stages. It was chosen as the formation of NRs should be the slowest, giving us a better chance to observe the occurring changes.

Samples: We took aliquots during the Cd and S precursors' injection phase (5 min, 10 min, 15 min), and during the growth phase (counted from the end of the Cd and S precursors mixture addition, 1, 3, 5, 7, 9, 11, 13, 15, 20, 30, 90 min).

Purification: Samples were centrifuged to remove the possibly formed sludge, and next purified by precipitating nanocrystals with ethanol, centrifugation, removing the supernatant containing the organic matter, and redispersing nanocrystals in hexane. In this process of purification up to 4 fractions were collected (please refer to the main text for details) and fraction 2 was analyzed. This allowed us, e.g., to remove PbS spherical particles formed during the reaction.

Measurements: Samples were examined with UV-Vis and PL spectroscopy; selected samples were additionally examined using TEM (5, 15 min of injection, 1, 20, 60, 120 min of growth).

TEM: During the injection phase we first noted the formation of nanocrystals with a distribution of sizes, some resembling initial perovskites (5 min of injection). Then, anisotropic and spherical nanoparticles appeared (presumably CdS and PbS, respectively, within 15 min of injection). During the growth phase, we removed PbS particles by centrifugation, revealing the presence of CdS nanocrystals with more and more well-defined anisotropic shapes in the course of the reaction. After 20 min of the growth phase, we were able to identify tetrapodic structures (side length 6.7± 1.0 nm), while later rod-like nanocrystals were revealed with dimensions 11.2±1.1 by 5.2± 0.6 nm (after 60 min of growth) and 16.0±1.8 nm by 5.2±0.7 nm (after 120 min of growth).

Regarding the measured shapes and sizes of nanocrystals, it is worth noting that: (a) NRs have triangular cross-section, which could suggest they appear by the overgrowth of the tetrapods, (b) the tetrapod side length and NRs are similar, with small differences may result from measurement bias and slow growth of the NRs in width, (c) the width of the NRs is almost constant during the reaction, indicating that the reaction proceeds by elongation of the long axis of the initially formed rods. This is in agreement with our previous conclusions that the CdS NRs growth occurs mainly in the six-fold axis direction, as shown by HR-TEM and XRD (Figure 2 in the main text).

UV-Vis: During the injection phase an absorption band appeared at ~400 nm (5 min of injection phase), red-shifting, and decreasing intensity (10 and 15 min of injection phase, Fig. S12). This is in agreement with the formation of small CdS nanocrystals. During the growth phase, the band further red-shifts, while increasing intensity, characteristic to growing particles and structural elongation.

PL spectra: a continuous red-shift of the emission band is revealed for consecutive samples both during the injection and growth stages; all measured samples exhibit a broadened FWHM

of the emission peaks in comparison to the initial dispersion of perovskites (Fig S13); these results are consistent with the formation and growth of CdS nanocrystals.

II. A control reaction without the use of perovskite nanocrystals (Fig. S14, S15).

To clarify whether perovskites play a key role in the process of CdS NRs formation, we performed a control synthesis. It included all substrates and solvents. The mixture was suspended in OAm, ODE, and OA, and heated up to 150 °C. Then, the mixture of the Cd/S precursors was added, and the reaction was carried out for two hours. We analyzed the products using TEM, UV-Vis, and PL spectroscopy after the purification procedure analogous to the original recipe.

TEM images revealed the formation of small (4.6± 0.4 nm diameter), mostly spherical nanocrystals. A minute amount of nanoparticles twice that size was also noted, seemingly formed by the coalescence of the main product. Most importantly, NRs were not found in the sample. The formed particles exhibit an absorption band slightly blue-shifted, compared to the NRs, while they do not exhibit photoluminescence in the vis range. We can thus conclude that perovskite nanocrystals are essential to the CdS NRs formation, at least regarding controlling the shape and size of nanocrystals. The smaller size of particles formed without the use of perovskites could suggest that the number of crystallization points is larger than when perovskites are present. We can thus reason that perovskite can limit the number of crystallization points by acting as seeds.

It should be noted, that results presented in Fig. S14b and Fig. S15b were achieved using lead (II) bromide in the amount corresponding to the full disintegration of perovskite nanocrystals. Analogous results were obtained if cesium oleate was used in place of lead (II) bromide. Thus, we conclude that the presence of bromide or cesium ions,[1] did not cause the CdS NRs formation, highlighting the role of perovskite nanocrystal presence in the reaction mixture.

III. The mechanism of CdS NR growth

Overall, we believe that at the initial stage of the synthesis, a gradual decomposition of perovskite nanocrystals occurs - small perovskite nanocrystals quickly disintegrate. The perovskite nanocrystals and their disintegrated parts can act as seeds for the growth of CdS nanoparticles. CdS nanoparticles first adopt a tetrapodic shape. Further growth of the tetrapods is mainly along the hexagonal axis, ultimately leading to nanorods with a

triangular/hexagonal cross-section. These claims are supported by the mentioned new experiments, TEM/XRD measurements, and comparison of NR cross-section, which is similar in size and shape to the tetrapods.

We can thus summarize, that the presence of perovskite nanocrystals is essential for the NRs formation, although our experiments do not disclose the quantitative effect of their partial disintegration. The process can occur via cation exchange, although it may also be partially be influenced by the presence of bromide and cesium ions in the reaction mixture.

IV. The influence of temperature and time of reaction (Fig. S8, S9).

The above conclusions (point III) are well documented for synthesis conducted at 150°C over 120 min. The influence of time and temperature can be further interpreted by analyzing the outcome of NC1-NC6 reactions given the above-mentioned conclusions.

a) NC1: reaction confirmed that after 20 min of reaction at 150°C tetrapod-like nanocrystals formed, thus, products of this synthesis are not included in Fig. S8 and S9.

b) NC2, NC3: Keeping the time and increasing the temperature to 180 °C and 230 °C, resulted in the formation of CdS NRs. These results evidence that increasing the temperature in comparison to NC4, increases the speed of tetrapod formation and overgrowth. The downside is that the product is less unfirm. In both cases the aspect ratio of NRs is ~2.7; higher temperature means larger NRs.

c) NC5, NC6: In comparison to NC2, NC3, and NC4, the 120 min long reactions at 200 °C and 250 °C result in products with notably smaller aspect ratios, while they have similar lengths compared to the product NC3 (Fig S8). Since in both cases, NRs are formed already after 20 min of reaction (as can be concluded from NC2 and NC3 reactions) the rest of the growth phase is reshaping the products. The observed morphological changes can occur via, e.g., the mechanism of digestive / Ostwald ripening or atom migration within a single crystal.

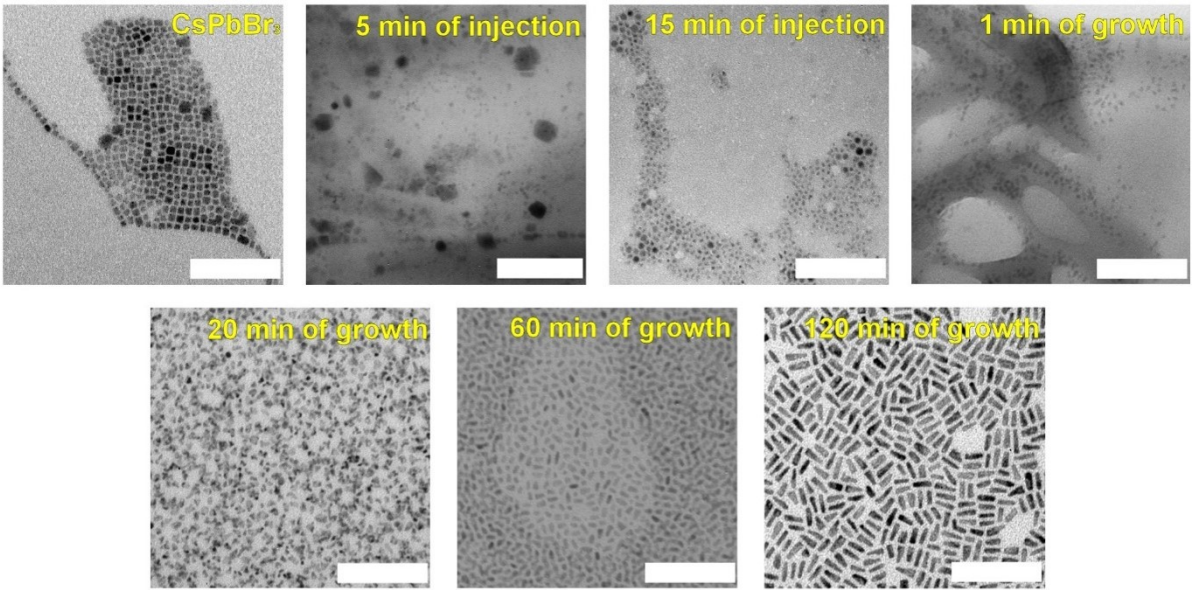

Fig. S 11 TEM images of nanoparticles obtained during the synthesis of NRs. Aliquots were taken in the following time intervals: 5, 15 min of injection, 1, 20, 60, 120 min of growth. The scale bar on each image is equal to 100 nm.

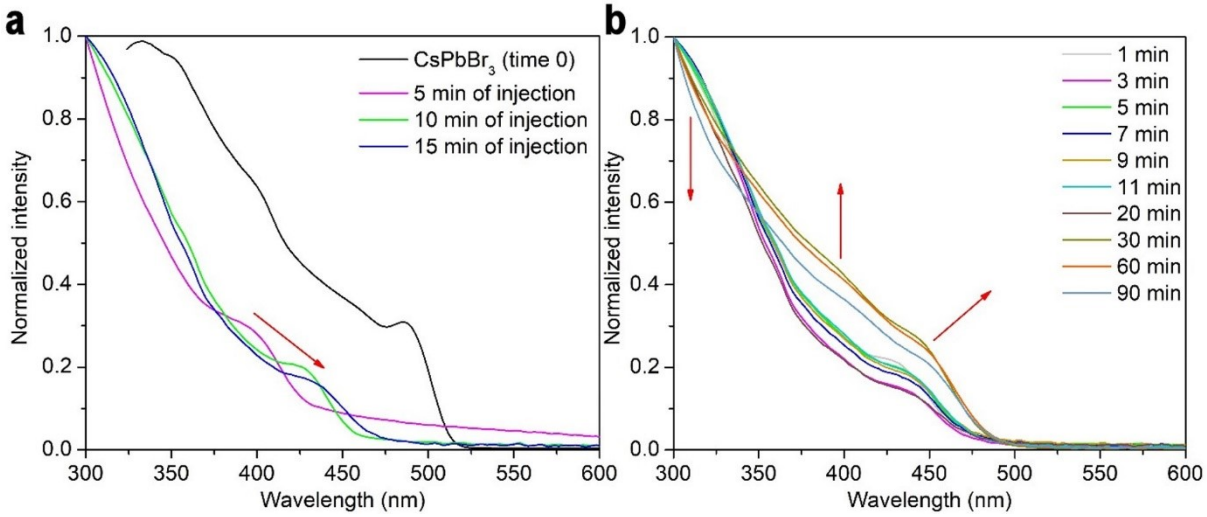

Fig. S 12 Normalized UV-Vis spectra of the aliquots taken during the NRs' synthesis. (a) change of the absorption in the course of the Cd and S precursor. (b) change of the absorption during the growth of the NRs. Red arrows present the change of the absorption band with the time of the reaction.

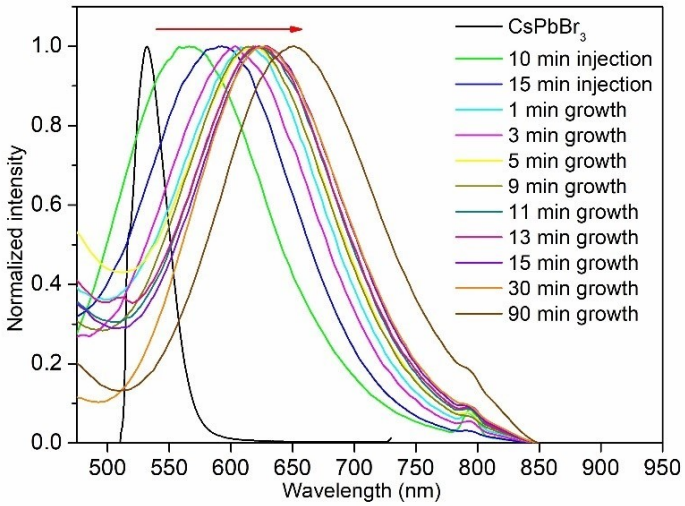

Fig. S 13 PL spectra of the aliquots taken during the NRs' synthesis. During the formation of nanorods, the PL peak shifts to the longer wavelengths.

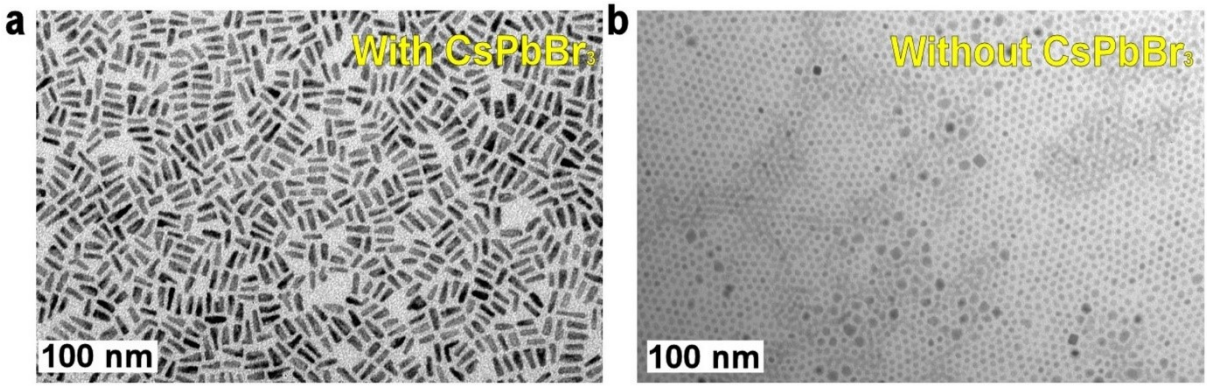

Fig. S 14 TEM images of (a) NC4 synthesized with the standard protocol. (b) with the omission of the first step, in which perovskites are obtained. It should be noted that bromide ions were added to the reaction mixture. Two types of nanocrystals have an average diameter 4.6 ±0.4 nm, and a small amount of larger (8.8± 0.8 nm) nanoparticles. No NRs are presented in the sample, which means perovskites are fundamental for the synthesis of rod-like CdS nanocrystals.

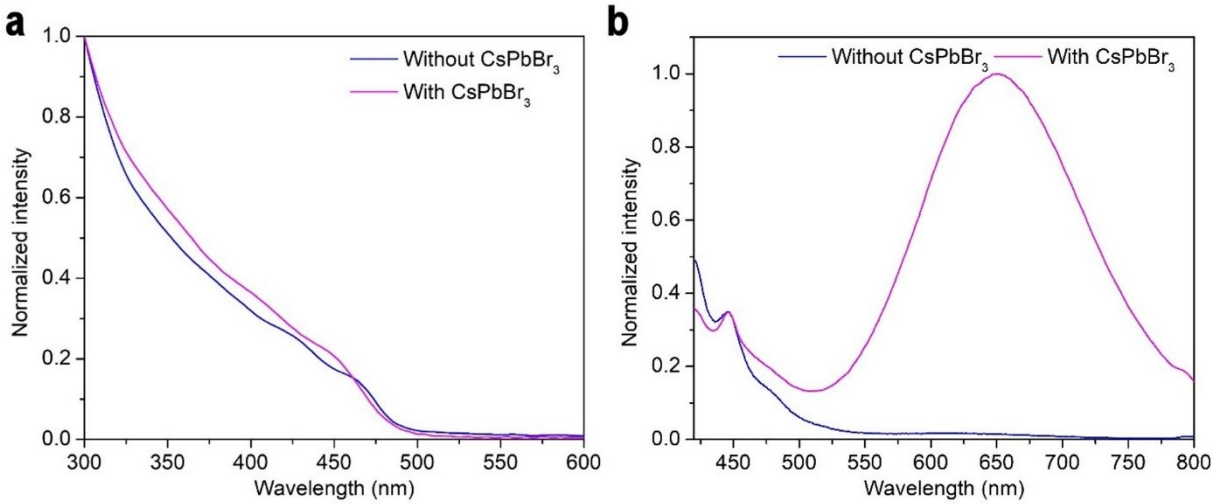

Fig. S 15 Comparing the optical properties of the nanoparticles obtained without $CsPbBr_3$ and reported NRs. (a) UV-Vis spectra. (b) PL spectra. The nanoparticles obtained without perovskites do not exhibit photoluminescence.

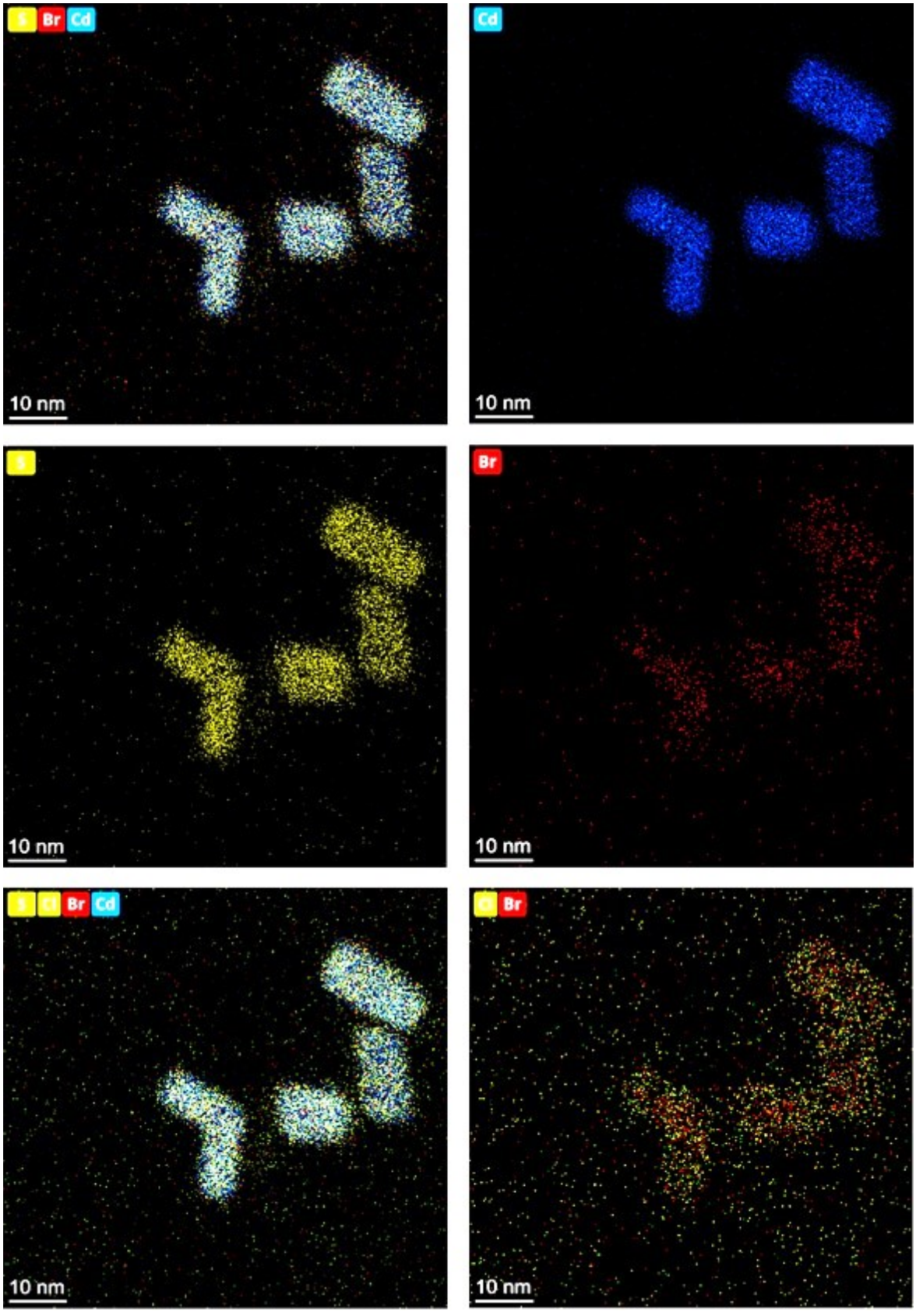

EDS-HAADF TEM elemental mapping

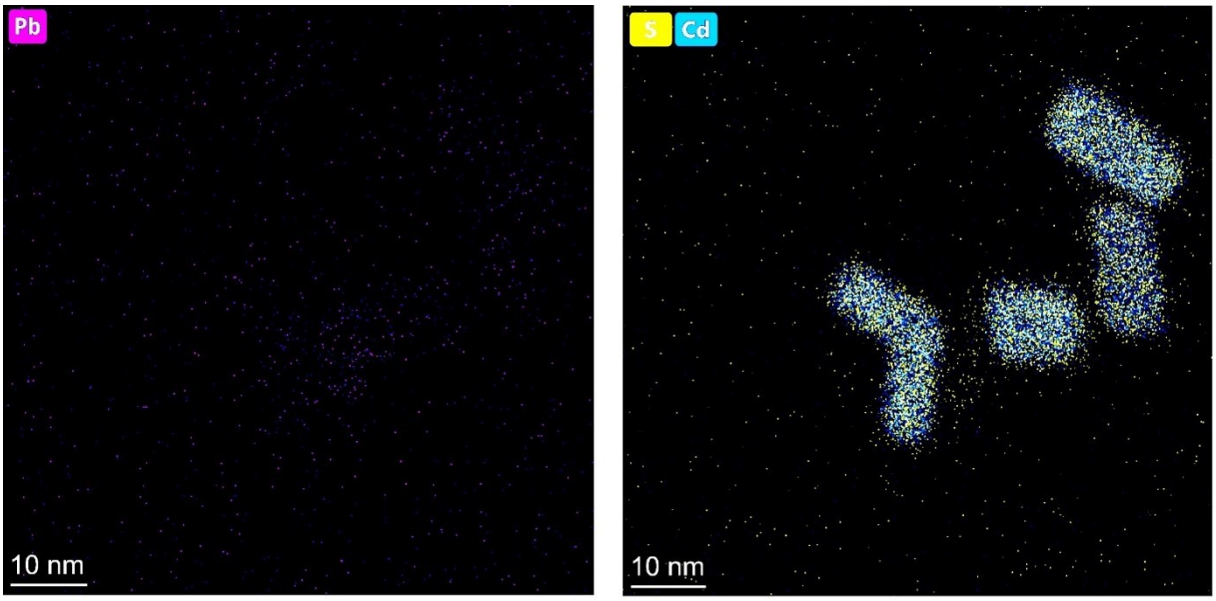

Fig. S 16 EDS-HAADF TEM elemental mapping of CdS NRs. The analysis does not show a significant presence of Pb atoms. The right bottom image (Cl, Br), shows the presence of Br only in the central, inert part of NRs, while Cl is uniformly distributed over the NRs, suggesting adsorption on the surface. Additionally, no significant accumulation of Pb can be co-localized with NRs.

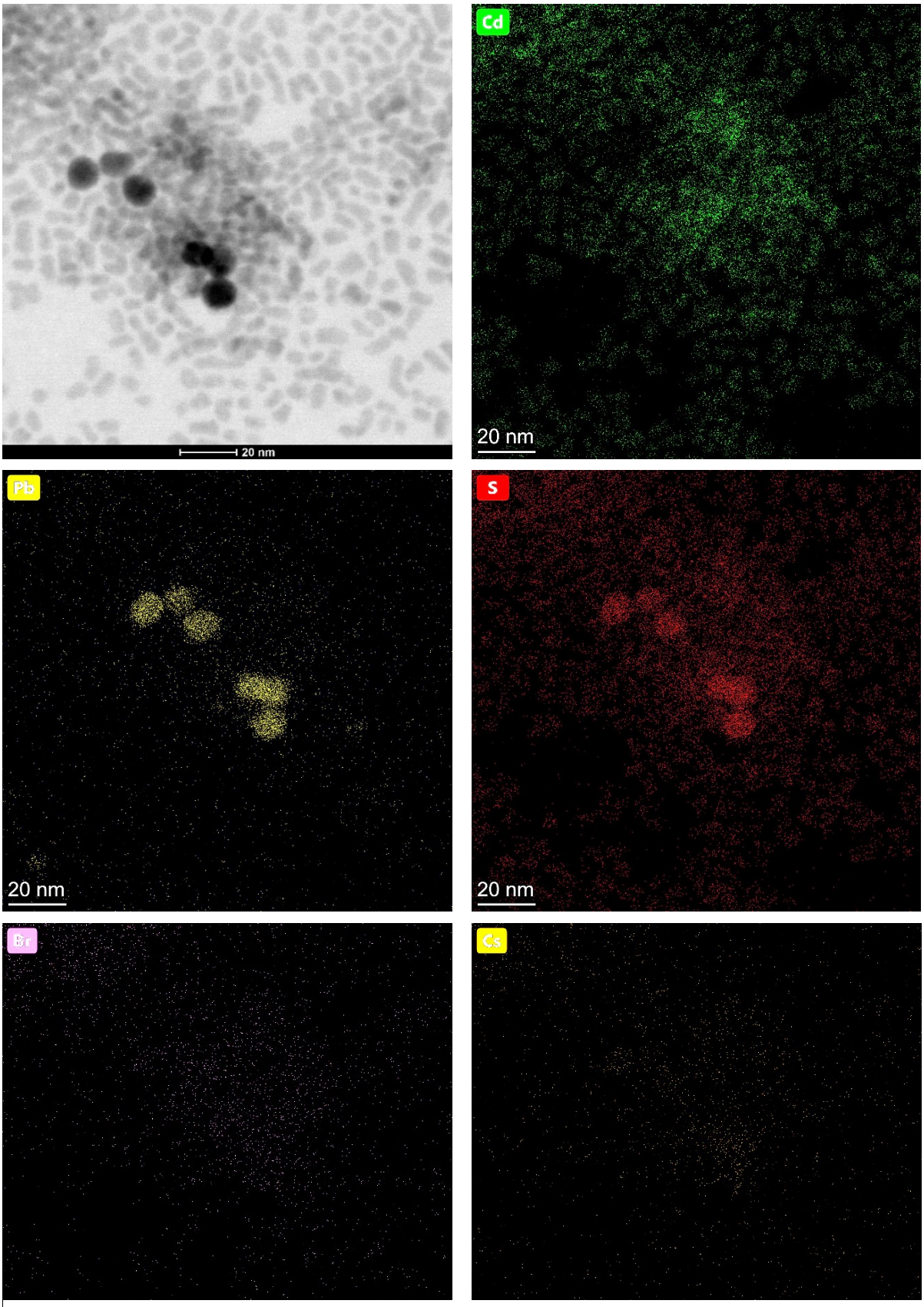

Fig. S 17 EDS elemental analysis of spherical nanoparticles co-formed in NC4 synthesis and the corresponding TEM image. The analysis reveals that these particles are PbS nanocrystals.

Stability of CdS NRs

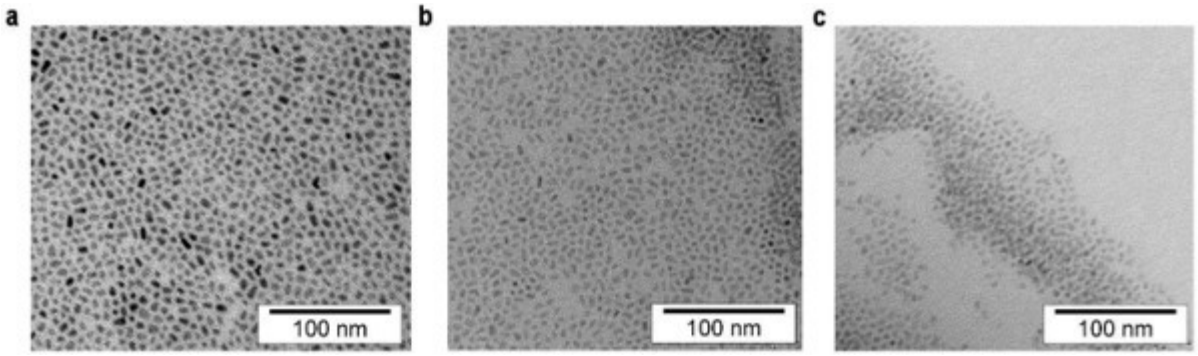

Fig. S 18 TEM images illustrate the stability of CdS NRs. (a) freshly synthesized NRs. (b) NRs stored for 4 weeks under nitrogen. No significant changes in NRs morphology can be observed. (c) NRs storage for 4 weeks under air atmosphere. Partial decomposition of NRs occurred.

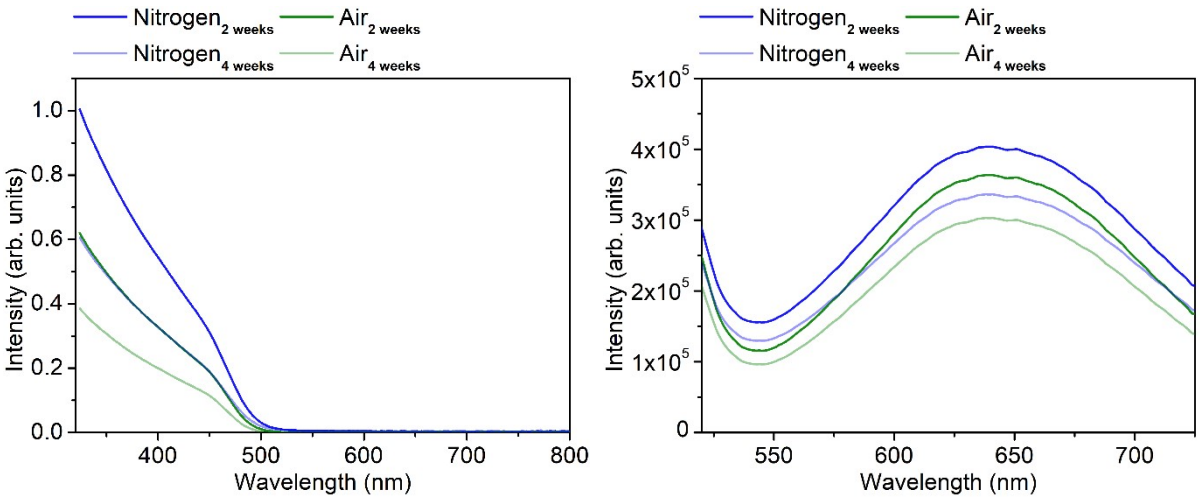

Fig. S 19 Absorption (left) and photoluminescence (right) spectra of the CdS NRs storaged under air and nitrogen atmosphere for 2 and 4 weeks.

Supplementary note 2. Formation of helical assemblies

The key to explaining how NRs are arranged on helices lies in the way the matrix crystallizes. Once the growth of the helical nanostructures is initiated, they can drive the assembly of NRs into helical configurations. During this process, NRs are expelled from the sample bulk to the air/fiber boundary. This effect could be ascribed to the reported tendency of NRs to locate at

the phase boundaries/defects of LC materials.[2,3] The edge of a nanofilament is a topological defect that increases the energy of the system. Clustering of NRs at the edges lowers the total energy of the system, probably by decreasing the molecular order at the fiber edges, caused by the admixing of mesogenic molecules from the NRs grafting layer. Selective placement of NRs at the sides of the twisted nanoribbons could be also favored by the specific interactions between the oleyl chain in the NRs organic coating ligands and OIM molecules located at the nanofiber sides. The long axes of OIM side chains are slightly tilted from the normal to the twisted layers that they form, while the ligands of NRs can bundle to follow this configuration. This effect was confirmed with XRD for Au nanoparticles.[4] It was also shown, that the chemical compatibility between the coating ligand and OIM molecule is necessary for the proper nanoparticle alignment on the helical nanofiber.

Bibliography

1 S. Ghosh and L. Manna, *Chem Rev*, 2018, **118**, 7804–7864.

2 M. A. Gharbi, S. Manet, J. Lhermitte, S. Brown, J. Milette, V. Toader, M. Sutton and L. Reven, *ACS Nano*, 2016, **10**, 3410–3415.

3 P. van der Asdonk and P. H. J. Kouwer, *Chem Soc Rev*, 2017, **46**, 5935–5949.

4 M. Bagiński, M. Tupikowska, G. González-Rubio, M. Wójcik and W. Lewandowski, *Advanced Materials*, 2020, **32**, 1904581.